


# Canard Mechanism and Rhythm Dynamics of Neuron Models

Feibiao Zhan <sup>1,\*</sup> , Yingteng Zhang <sup>2</sup>, Jian Song <sup>3,4</sup> and Shenquan Liu <sup>3</sup><sup>1</sup> Department of Applied Mathematics, Nanjing Audit University, Nanjing 211815, China<sup>2</sup> Department of Mathematics, Taizhou University, Taizhou 225300, China<sup>3</sup> School of Mathematics, South China University of Technology, Guangzhou 510640, China<sup>4</sup> School of Mathematical and Computational Sciences, Massey University, Auckland 4442, New Zealand

\* Correspondence: feibiu.zhan@nau.edu.cn

**Abstract:** Canards are a type of transient dynamics that occur in singularly perturbed systems, and they are specific types of solutions with varied dynamic behaviours at the boundary region. This paper introduces the emergence and development of canard phenomena in a neuron model. The singular perturbation system of a general neuron model is investigated, and the link between the transient transition from a neuron model to a canard is summarised. First, the relationship between the folded saddle-type canard and the parabolic burster, as well as the firing-threshold manifold, is established. Moreover, the association between the mixed-mode oscillation and the folded node type is unique. Furthermore, the connection between the mixed-mode oscillation and the limit-cycle canard (singular Hopf bifurcation) is stated. In addition, the link between the torus canard and the transition from tonic spiking to bursting is illustrated. Finally, the specific manifestations of these canard phenomena in the neuron model are demonstrated, such as the singular Hopf bifurcation, the folded-node canard, the torus canard, and the “blue sky catastrophe”. The summary and outlook of this paper point to the realistic possibility of canards, which have not yet been discovered in the neuron model.

**Keywords:** canards; neuron model; singular perturbation system; transient dynamics; discharge; rhythm transition

**MSC:** 68Q99; 34D15; 34E17



**Citation:** Zhan, F.; Zhang, Y.; Song, J.; Liu, S. Canard Mechanism and Rhythm Dynamics of Neuron Models. *Mathematics* **2023**, *11*, 2874. <https://doi.org/10.3390/math11132874>

Academic Editors: Dimplekumar N. Chalishajar, Valery G. Romanovski and Rodica Luca

Received: 11 March 2023

Revised: 26 May 2023

Accepted: 25 June 2023

Published: 27 June 2023



**Copyright:** © 2023 by the authors. Licensee MDPI, Basel, Switzerland. This article is an open access article distributed under the terms and conditions of the Creative Commons Attribution (CC BY) license (<https://creativecommons.org/licenses/by/4.0/>).

## 1. Introduction

The canard was discovered while researching the relaxation oscillation in the two-dimensional plane [1–3]. Dynamic behaviours caused by canards have been intensively studied and debated in terms of mathematical theory and applications for the last three decades [4]. Generally, a canard is a transient dynamic phenomenon in multi-time-scale systems (singularly perturbed systems) and is a particular class of solutions with various dynamic behaviours in the boundary region of the system [5–8]. In other words, the solution follows an attracting slow manifold, passes through a bifurcation point on the critical manifold (for  $\varepsilon = 0$ ) and then follows a repelling slow manifold for a long time [9]. It is quite difficult to witness it directly in experiments (so-called canard explosion) due to the sensitivity of the system parameters [10]. Furthermore, the phase-space geometry of some canard cycles has been found in the van der Pol system [10,11], which is similar to that of a duck, so a canard is also called a “duck” [1,2,12–16]. Researchers are still investigating it using matched asymptotic expansions [17,18] and the geometric singular perturbation theory [19,20]. The explosion method extends the geometric singular perturbation theory to non-hyperbolic points to analyse the dynamics near the system fold [12,19–21]. Dumortier et al. used the singular explosion and centre manifold approaches to provide a geometric explanation and proof of a duck solution’s cycles, which

was a breakthrough in geometric theory [19]. For specific explosion methods, the reader can refer to the literature [22,23].

The explosion method extends a large number of theoretical results in the application of two-dimensional singular perturbation problems, including canards, folds, canard explosions, relaxation oscillation, and other related theories and concepts [20,24–26]. Sz-molyan et al. used the explosion method to show the geometric analysis of degenerate singularities (non-hyperbolic points) on the fold curve of a three-dimensional system and explained the existence of a canard at the saddle, folded node and folded saddle [12,21]. Of course, canards also exist in high-dimensional system [10]. The geometric singular perturbation theory is derived from Fenichel's theory, a geometric theory of multiscale dynamic systems [27–30]. A theoretical analysis was expounded about its specific application in canards [9]. It was developed from the numerical simulation and expansion of the canard in fast/slow dynamic systems [31,32].

In this paper, the singular perturbation problem under general conditions is introduced. The initial discussion on the canard is about the case of a folded node and folded saddle. Researchers have specifically explored and studied a vast variety of analyses at the folded node [4,33–38]. The faux canard theory at the folded saddle, the role of folded-saddle canards in parabolic bursters, and the relationship between folded canards and the firing-threshold manifold have been discussed [6,39,40]. In recent years, researchers have studied the local dynamics around the folded-saddle singularity and analysed canards of folded saddle type I and type II [12,38,41–44]. Brøns et al. analysed mixed-mode oscillations (MMOs) caused by the canard and singular Hopf bifurcation in a forest pest model [45,46]. Moreover, a theoretical analysis of the torus canard was also discussed [13–15,47]. Some researchers have been attempting to demonstrate the impact of fast/slow torus systems on plane systems [13]. The relationship between the analysis of the torus canard and the firing-mode transition of a neuron has also been introduced [48–55]. The transition between the single spiking and burster mode of the neuron model has been explained by integrating the concepts of average field, folded singularities, and the torus canard [56].

Canards exist in neuron models, chemical models, circuit models, etc. The concept of the canard has been used in numerous areas, such as the effect of the canard on system excitability [57,58], and the location of the canard explosion can be provided [59]. The canard mechanism has been applied to analyse the dynamic behaviours of synchronous and asynchronous neuron firing [60–62]. Canards emerge in the piecewise-linear, continuous, slow-fast dynamical system [4,63–65]. Many neuron models and nonlinear systems have explained the interaction between MMOs and canards [33–35,66,67]. Canards and hidden canards exist in simplified Hodgkin–Huxley neuron models [68,69]. Researchers have employed random perturbations and topology to analyse the mechanism of canards [70,71], and the feedback control of canards has also been studied [72].

Nerve impulse production and transmission are critical components of neural information encoding. However, they do not represent the entirety of nerve signals, and the subthreshold behaviour of neurons is critical for parsing the input of nerve signals [73]. Analysing nerve signals can be aided by understanding the dynamic behaviour of neuronal firing rhythms. As a result, not only should single spiking, burster and MMO neurons be studied, but also the information contained in the transient transitions between them. We are interested in interpreting the dynamic behaviour of neuronal firing rhythms.

Since the groundbreaking Hodgkin–Huxley neuron model has been proposed [74–77], a large number of simplified models based on this classical model have been presented, such as the FitzHugh–Nagumo [78,79], Morris–Lecar [80], Hindmarsh–Rose [81] models, etc. Rinzel et al. retained the fast/slow structure of the system and simplified the Hodgkin–Huxley model to a two-dimensional system. By assuming the variable  $m$  was in equilibrium and finding that  $n$  and  $h$  were almost in a linear relationship, the simplified model was obtained, and a theoretical analysis was conducted [82]. Further, Rinzel used the fast/slow dynamics method for the first time to perform a systematic theoretical analysis of the dynamic mechanism of neuronal discharges [83] and proposed the parabolic burster [84].

Later, this method was widely extended to analyse neuronal discharges and was used to explain many types of burster discharges. For example, a square-wave burster mechanism was proposed [85], an elliptic burster mechanism was presented [86], the mechanism of taper bursters was analysed [87,88], and the generation mechanism of triangular bursters was discussed [89–91]. Izhikevich considered bifurcations of the resting state and active state of the burster and proposed a relatively comprehensive theoretical classification method, namely a “top-down” fast/slow dynamics bifurcation analysis [92–94]. It allowed a comprehensive analysis and explanation of various bifurcation mechanisms of discharge rhythm in the fast/slow neuron model [95–99].

The MMOs are special kinds of bursting mode of neurons, which is a mixed rhythm of superthreshold oscillations and subthreshold ones. A recent review summarizes the pioneering work of Rinzel and Izhikevich on bursting patterns’ classification of excitatory systems and proposes a canard mechanism for folded-node singularities, explaining that conductance-based MMOs consist of subthreshold and superthreshold oscillations [100]. Canards have been the subject of active study since it was proposed in the 1980s, and they have been used to understand the firing patterns of neurons [101–104]. Canards are closely related to synchronization, spiking–adding, and complex oscillations of excitation networks [105–107]. A detailed theoretical elaboration is summarized in the literature [108,109], and geometric singular perturbation theory has also been applied to a model of calcium dynamics [110]. The mathematical mechanism of MMOs has several explanations, including the slow passage of the solution trajectory through the singular Hopf bifurcation [87,111–114], the fracture of the invariant torus [115], the instability of the Shilnikov homoclinic orbit [116,117], the subcritical Hopf bifurcation [118,119], and so on. The link between MMOs and canards has been investigated [120]. Among them, Lu et al. paid attention to the relationship between MMOs and canards in a neuron model [121]. They introduced the definition of MMOs and showed MMOs in a neuron model as well as the theoretical conclusions of the interaction among canards. Since the relationship between canards and MMOs was first discovered in the neuron model [1,17], the potential connection between the two has been revealed and proven [33–35,46,66,122,123]. The bursting mode of neurons is strongly connected with the canards of folded singularities. For example, the canard of folded nodes can cause MMOs [33,34,123] and the folded saddle is closely related to the parabolic burster and the firing-threshold manifold [39,47]. The torus canard is related to the transition from single spiking to bursting [52,54,55] and so on. The firing mechanism of the neuron model is adequately explained by the canard theory. That is, it not only has comparable numerical findings, but also theoretically explain these results. As a result, the canard theory provides an effective processing tool for explaining the discharge mechanism of the neuron model. Neuronal firing rhythm research is still ongoing. To summarise, it is necessary to pay attention to the transient transition of rhythm between spiking modes, between spiking and bursting modes, and between bursting modes. This work describes the link between the canard phenomenon and neuron firing, as well as their transient transition dynamics.

The rest of this review is organized as follows. Section 2 presents some conclusions of the geometric singular perturbation theory. Section 3 gives some theorems and calculation methods of singular canards. They are then used to introduce the relationship between canards and the rhythm discharge of the neuron model in Section 4.

## 2. Geometric Singular Perturbation Theory

We first give some results on canards and folded singularities in Sections 2 and 3, which are used later in the discussion of the rhythmic firing dynamics of neurons. Many neuron models have been analysed as systems on fast and slow time scales; hence, we consider the high-dimensional parameter system (1)

$$\begin{cases} w' = \varepsilon g(w, v, \varepsilon), \\ v' = f(w, v, \varepsilon). \end{cases} \quad (1)$$

where  $(w, v) \in R^n \times R^m$  is the state-space variable and  $n, m \geq 1$ . Variable  $v = (v_1, v_2, \dots, v_m)$  represents the fast variable, and variable  $w = (w_1, w_2, \dots, w_n)$  represents the slow variable. Moreover, the system representation takes the derivative with respect to time  $t$ ,  $\varepsilon \ll 1$  is a small positive parameter, which indicates the difference in the time scale between the fast variable and the slow variable. Assume  $f, g$  is  $C^\infty$  smooth. After time-scale transformation  $\tau = \varepsilon t$ , the slow time-scale system is obtained as follows (2):

$$\begin{cases} \dot{w} = g(w, v, \varepsilon), \\ \varepsilon \dot{v} = f(w, v, \varepsilon). \end{cases} \quad (2)$$

The dot denotes taking the derivative with respect to time  $d/d\tau$ .

The regular perturbed system is the solution with no significant difference when the small parameter approaches zero or equals zero [124]. Furthermore, we call systems (1) and (2) singularly perturbed systems, that is, the solution of the degenerate system is fundamentally different from that of the original system. We want to use the idea of regular perturbation to understand the singular perturbation problem as theoretically as possible. When  $\varepsilon \rightarrow 0$ , the trajectory of system (1) converges to the solution of the  $m$ -dimensional layer (fast) problem during the fast-fibre segment (3):

$$\begin{cases} w' = 0, \\ v' = f(w, v, 0). \end{cases} \quad (3)$$

In the slow segment, the trajectory of system (2) converges to the solution of system (4) as follows:

$$\begin{cases} \dot{w} = g(w, v, 0), \\ 0 = f(w, v, 0). \end{cases} \quad (4)$$

The differential-algebraic problem is called the reduced (slow) problem. The idea of the geometric singular perturbation theory is to predict the dynamics of the whole system, (1) or (2), by combining low-dimensional subsystems (3) and (4) [27,30].

### Layer Problem (3)

The slow variable  $w$  is the parameter of the system. Its set of equilibrium points is expressed as  $S := \{(w, v) \in R^n \times R^m | f(w, v, 0) = 0\}$  and it is called a critical manifold.

**Definition 1** ([9]). We say that subset  $S_h \in S$  is a normally hyperbolic manifold if the Jacobian  $D_v f$  with respect to the fast variable  $v$  does not have any eigenvalue with a zero real part, that is, for all  $(w, v) \in S_h$ , it is the hyperbolic equilibrium point of the layer problem.  $S_h$  is called attracting if the eigenvalues of the Jacobian matrix all have negative real parts; if all the eigenvalues of the Jacobian matrix have positive real parts,  $S_h$  is called repelling; if  $S_h$  is neither attracting nor repelling, it is called saddle-shaped.

**Definition 2** ([10]). If the Jacobian  $D_v f$  has at least one eigenvalue with a zero real part (non-normal hyperbolic) on  $S_h$ , then the layer problem is bifurcated. Given the definition of a fold [9,125], the critical manifold of singularly perturbed system (2) has a (local) fold structure. If there is a set  $F$ , which constitutes an  $(n-1)$ -dimensional manifold on an  $n$ -dimensional critical manifold, it is defined as:  $F := \{(w, v) \in R^k \times R^m | f(w, v, 0) = 0, \text{rk}(D_v f)(w, v, 0) = m-1, l \cdot [(D_{vv}^2 f)(w, v, 0)(r, r)] \neq 0, l \cdot (D_w f)(w, v, 0) \neq 0\}$ .  $l$  and  $r$  correspond to vectors in the null space of Jacobian  $D_v f$ , which defines the set of critical manifold fold points and the set  $F$  provides the possibility of canards.

**Definition 3** ([9]). For the normally hyperbolic critical manifold  $S_h$ , the locally stable and unstable manifolds are denoted as  $W_{loc}^s(S_h)$  and  $W_{loc}^u(S_h)$  and expressed as  $W_{loc}^s(S_h) = \bigcup_{p \in S_h} W_{loc}^s(p)$  and  $W_{loc}^u(S_h) = \bigcup_{p \in S_h} W_{loc}^u(p)$ , respectively.  $W_{loc}^s(p)$  and  $W_{loc}^u(p)$  constitute the fast-fibre families of  $W_{loc}^s(S_h)$  and  $W_{loc}^u(S_h)$  based on  $p$ , respectively (called a fast fibration or foliation).

The geometric singular perturbation theory of normally hyperbolic manifold is called Fenichel's theory [9,27,30]. This theory guarantees the existence of normal hyperbolic manifolds approximating  $S_h \in S$ , and the theorems on the corresponding locally stable and unstable manifolds approximating  $W_{loc}^s(S_h)$  and  $W_{loc}^u(S_h)$  are as follows:

**Theorem 1** (Fenichel's Theorem 1, [9,27,30]). Given system (1) with  $f, g \in C^\infty$ , suppose  $S_h \in S$  is a compact normally hyperbolic manifold (possibly with a boundary). For a sufficiently small  $\varepsilon > 0$ , the following holds:

- (i) For any  $r < \infty$ , there exists a  $C^r$ -smooth manifold  $S_{h,\varepsilon}$  (not necessarily unique, but exponentially approximating each other), locally invariant under flow (1), that is,  $C^r O(\varepsilon)$  approaches  $S_h$ .
- (ii) For any  $r < \infty$ , there exist  $C^r$ -smooth stable and unstable manifolds

$$W_{loc}^s(S_{h,\varepsilon}) = \bigcup_{p_\varepsilon \in S_{h,\varepsilon}} W_{loc}^s(p_\varepsilon), \quad W_{loc}^u(S_{h,\varepsilon}) = \bigcup_{p_\varepsilon \in S_{h,\varepsilon}} W_{loc}^u(p_\varepsilon),$$

locally invariant under flow (1), which are  $C^r O(\varepsilon)$  and approach  $W_{loc}^s(S_h)$  and  $W_{loc}^u(S_h)$ , respectively.

- (iii) The foliation  $\{W_{loc}^s(p_\varepsilon) | p_\varepsilon \in S_{h,\varepsilon}\}$  is (positively) invariant, that is

$$W_{loc}^s(p_\varepsilon) \cdot t \subset W_{loc}^s(p_\varepsilon \cdot t),$$

for all  $t \geq 0$  such that  $p_\varepsilon \cdot t \in S_{h,\varepsilon}$ , where  $t$  represents the solution operator for system (1).

- (iv) The foliation  $\{W_{loc}^u(p_\varepsilon) | p_\varepsilon \in S_{h,\varepsilon}\}$  is (negatively) invariant, that is

$$W_{loc}^u(p_\varepsilon) \cdot t \subset W_{loc}^u(p_\varepsilon \cdot t),$$

for all  $t \leq 0$  such that  $p_\varepsilon \cdot t \in S_{h,\varepsilon}$ , where  $t$  represents the solution operator for system (1).

#### Reduced Problem (4)

Describing differential algebra problems with slow variables  $w$  restricted to the critical manifold forms the following reduced problem (5):

$$\begin{cases} \dot{w} = g(w, v, 0), \\ -D_v f \cdot \dot{v} = (D_w f) \cdot g(w, v, 0). \end{cases} \quad (5)$$

where  $(w, v) \in S$ . Define  $\text{adj}(D_v f)$  as the adjoint matrix of  $D_v f$ , that is,  $\text{adj}(D_v f) \cdot D_v f = D_v f \cdot \text{adj}(D_v f) = \det(D_v f)I$ .

Multiply both sides of the second equation of system (5) by  $\text{adj}(D_v f)$  to obtain system (6):

$$\begin{cases} \dot{w} = g(w, v, 0), \\ -\det(D_v f) \cdot \dot{v} = \text{adj}(D_v f) D_w f \cdot g(w, v, 0). \end{cases} \quad (6)$$

where  $(w, v) \in S$ ; it provides an alternative form of reproduction for original system (4).

In order to distinguish the equilibrium point between system (6) and reduced system (4), two types of singularities are defined:

- (i) If  $g = 0$ , we call it a general singularity;
- (ii) If  $\det(D_v f) = 0$  and  $\text{adj}(D_v f) \cdot D_w f \cdot g = 0$ , we call it a folded singularity.



In general, the set  $M_f$  is regarded as the set of equilibrium points of system (6) [10]. It has  $(n - 2)$  zero eigenvalues and two eigenvalues  $\lambda_{1/2}$  with nonzero real parts. The classification of folded singularities is based on the two nonzero eigenvalues  $\lambda_{1/2}$  and follows the law of singularities in a two-dimensional vector field.

**Definition 4** ([9,12]). *The classification of the general folded singularity can be expressed as:*

- (i) *In the case where  $\lambda_{1/2}$  is a real number, denote the ratio as  $\mu := \lambda_1 / \lambda_2$ . Without loss of generality, assume  $|\lambda_1| \leq |\lambda_2|$ . The corresponding singularity is either a folded saddle if  $\mu < 0$ , or a folded node if  $0 < \mu < 1$ .*
- (ii) *If  $\lambda_{1/2}$  is complex conjugate and  $\text{Re}(\lambda_{1/2}) \neq 0$ , then the corresponding singularity is the folded focus.*

Assume that the critical manifold  $S$  is normally hyperbolic, that is,  $D_v f$  is full rank for all  $(w, v) \in S$ . The implicit function theorem states that  $S$  can be given by graph  $v = h(w)$ . System (6) can be given by (7) as follows:

$$\dot{w} = g(w, h(w), 0), \quad (7)$$

and the slow flow in  $S_{h,\varepsilon}$  continues to approximate the reduced flow in  $S_h$ . The theorem is as follows:

**Theorem 2** (Fenichel's Theorem 2, [9,27,30]). *Given system (1) with  $f, g \in C^\infty$ , suppose  $S_h \subseteq S$  is a compact normally hyperbolic manifold (possibly with a boundary). For a sufficiently small  $\varepsilon > 0$ , Theorem (1)(i) holds and the following is true:*

- (i) *The slow flow on  $S_{h,\varepsilon}$  converges to the reduced flow on  $S_h$  as  $\varepsilon \rightarrow 0$ . Since  $S_h$  is a graph  $v = h(w)$ ,  $S_{h,\varepsilon}$  is also a graph  $v_\varepsilon = h(w, \varepsilon)$  for a sufficiently small  $\varepsilon \ll 1$ . Thus, the slow flow on  $S_{h,\varepsilon}$  follows (8):*

$$\dot{w} = g(w, h(w, \varepsilon), \varepsilon). \quad (8)$$

We can deal with the regular perturbation problem on  $S_{h,\varepsilon}$ ; this is a remarkable result. Therefore, we obtain Lemma 1.

**Lemma 1.** *The hyperbolic equilibrium of reduced problem (7) as the hyperbolic equilibrium of total problem (2) is maintained for a sufficiently small  $\varepsilon \ll 1$ .*

The following theorem states that the stable manifold  $W^s(S_{h,\varepsilon})$  decays exponentially towards its corresponding base point  $p_\varepsilon \in S_{h,\varepsilon}$ , as does the trajectory of the unstable manifold  $W^u(S_{h,\varepsilon})$  in backward time.

**Theorem 3** (Fenichel's Theorem 3, [9,27,30]). *Suppose  $\lambda_i$  is a stable eigenvalue for the critical manifold  $S_h$  whose upper bound  $\alpha_s < 0$ , such that  $\text{Re}(\lambda_i) < \alpha_s < 0, i = 1, 2, \dots, m_s$ . There exists a constant  $k_s > 0$ , such that  $p_\varepsilon \in S_{h,\varepsilon}$  and  $q_\varepsilon \in W_{loc}^s(p_\varepsilon)$  yield  $\|q_\varepsilon \cdot t - p_\varepsilon \cdot t\| \leq k_s \exp(\alpha_s t)$ , which makes  $p_\varepsilon \cdot t \in S_{h,\varepsilon}$  true for all  $t \geq 0$ .*

Similarly, suppose  $\lambda_i$  is an unstable eigenvalue for the critical manifold  $S_h$  whose lower bound  $\alpha_u > 0$ , such that  $\text{Re}(\lambda_j) > \alpha_u > 0, j = 1, 2, \dots, m_u$ . There exists a constant  $k_u > 0$ , such that  $p_\varepsilon \in S_{h,\varepsilon}$  and  $q_\varepsilon \in W_{loc}^u(p_\varepsilon)$  yield  $\|q_\varepsilon \cdot t - p_\varepsilon \cdot t\| \leq k_u \exp(\alpha_u t)$ , which makes  $p_\varepsilon \cdot t \in S_{h,\varepsilon}$  true for all  $t \leq 0$ .

As can be seen from the above, the theorem ensures that the singular perturbation problem is transformed into a nonsingular perturbation problem.  $S_{h,\varepsilon}$  is an invariant manifold, a critical manifold approximation ( $O(\varepsilon)$  perturbation) for the layer problem. In the normally hyperbolic part of the critical manifold, the slow flow on the invariant manifold  $S_{h,\varepsilon}$  is connected with the reduced flow ( $O(\varepsilon)$  perturbation approximation  $S_{h,\varepsilon}$ ). That is, the dynamics of the  $K$ -dimensional invariant slow flow  $S_{h,\varepsilon}$  can be completely

described by the reduced flow  $S_h$ . Then, the dynamics of whole system (1) or (2) can be predicted by combining the low-dimensional subsystem layer problem and reduced problem. This clever dimensionality reduction method provides a good idea to explain the discharge mode and transition behaviour of a highly nonlinear neuron model.

### 3. Singular Canards

#### 3.1. Limit-Cycle Canard

##### 3.1.1. Singular Hopf Canards for Fast/Slow Time Scale Systems

Singular Hopf canards occur in fast/slow time-scale systems or systems essentially having a slow time scale. When a Hopf bifurcation occurs in a two-dimensional plane system, that is, a pair of pure imaginary eigenvalues at the equilibrium point pass through the imaginary axis at a nonzero speed with a parameter change [126], a canard explosion is prone to occur, that is, the amplitude of the periodic trajectory near the Hopf bifurcation increases rapidly. Periodic trajectories branching out of bifurcation points can be roughly divided into two categories: one is the category of stable periodic trajectories, which is called a supercritical Hopf bifurcation, and the other is the category of unstable periodic trajectories, called subcritical Hopf bifurcation. Their bifurcation type can be measured by the sign of the Lyapunov coefficient (except for a generalized Hopf bifurcation). There are many canard explosion dynamics of singular Hopf bifurcations associated with planar systems using geometric singular perturbation theory and asymptotic methods [17,20,26]. These results can be summarized as follows:

**Theorem 4** ([120]). *Given system (1) with  $f, g \in C^\infty$  ( $m = 1, n = 1$ ), and  $S$  denotes the critical manifold, assume that the plane fast/slow system has a general fold  $\bar{p} = (w_0, v_0) \in S$ , that is, it satisfies:*

$$f(\bar{p}, \lambda, 0) = 0, \frac{\partial f(\bar{p}, \lambda, 0)}{\partial v} = 0, \frac{\partial^2 f(\bar{p}, \lambda, 0)}{\partial v^2} \neq 0, \frac{\partial f(\bar{p}, \lambda, 0)}{\partial w} \neq 0.$$

*Suppose the critical manifold is locally attracting at  $v < v_0$  and repelling at  $v > v_0$ , and there is a folded singularity at  $\bar{p}$  when  $\lambda = 0$ , that is,*

$$g(\bar{p}, 0, 0) = 0, \frac{\partial g(\bar{p}, 0, 0)}{\partial v} \neq 0, \frac{\partial g(\bar{p}, 0, 0)}{\partial \lambda} \neq 0.$$

*Then, a singular Hopf bifurcation and a canard explosion appear in*

$$\lambda_H = H_1 \varepsilon + O(\varepsilon^{3/2}) \text{ and } \lambda_c = (H_1 + K_1) \varepsilon + O(\varepsilon^{3/2}).$$

*The coefficients  $H_1$  and  $K_1$  can be clearly calculated by the transformation of the canonical form [20], or the first-order Lyapunov coefficients of the Hopf bifurcation can be considered [59].*

The intersection line of the maximal canard corresponding to the  $\varepsilon$  neighbourhood of the attracting manifold and the  $\varepsilon$  neighbourhood of the repelling manifold extend the flow of system (1) into the neighbourhood of the set of singularities. The maximal canard defines a family of canards whose exponents approximate the maximal canard. That is, the solution trajectory of system (1) follows the attracting neighbourhood of the slow flow toward the neighbourhood of the singularity set and after passing the singularity set, follows the repelling neighbourhood of the slow flow for a long period of time. Due to the nonuniqueness of the neighbourhood, such a family of canards is presented as the unique singular canard in the singular limit  $\varepsilon \rightarrow 0$ . In other words, singular perturbed systems have critical manifolds with fold singularities, and the trajectory of the reduced system reaches the repelling branch (manifold) in a finite time from the attracting branch (manifold) of the critical manifold through the fold singularity, which is called the singular canard. If the system trajectory from the repelling branch near the singularity goes through

the singularity to the attracting branch in a finite time, we call this solution orbit the singular faux canard. In simple terms, the canard from the attracting critical manifold to the repelling critical manifold is a canard without a head, and the canard from the attracting critical manifold to another attracting branch through the repelling branch is a canard with a head. Specific examples of the singular Hopf canard explosion in the neuron model is given in the next section.

### 3.1.2. Singular Hopf-like Bifurcation for Systems with One Time Scale

The MMOs of neuron models caused by a subcritical Hopf bifurcation on a single time scale can be observed [119]. To describe the process briefly: in the process of the equilibrium point  $q$  (deep) passing through the subcritical Hopf bifurcation to the saddle focus, the stable manifold trajectory near  $q$  flows into it, and then the slow spiral simultaneously increases the amplitude away from  $q$  (the whole process is very similar to the singular Hopf bifurcation). The reason is that the centre manifold of the  $q$  point's subcritical Hopf bifurcation has a weak instability, and the global regression mechanism has a strong robustness. The trajectory of the system near  $q$  is likely to cause a long period of small increasing amplitude oscillations. In this way, if the spiral wave trajectory returns to the neighbourhood of  $q$  by the global regression mechanism, MMOs are generated. In fact, the Hopf bifurcation essentially introduces a slow time scale, which is related to the real part of the unstable complex eigenvalues. Examples of three-dimensional fast/slow systems and high-dimensional fast/slow systems have been analysed [118,119].

### 3.2. Folded Singular Canards for Fast/Slow Time Systems

Given a particular system that has one fast variable and two slow variables, i.e.,  $m = 1$ ,  $n = 2$ , the system can be expressed as (9):

$$\begin{cases} w' = \varepsilon g_1(w, u, v, \varepsilon), \\ u' = \varepsilon g_2(w, u, v, \varepsilon), \\ v' = f(w, u, v, \varepsilon). \end{cases} \quad (9)$$

where  $w, u, v$  represent one-dimensional variables. After the corresponding treatment of the reduced problem of system (9), desingularized system (10) is obtained as follows:

$$\begin{cases} \dot{w} = -\det(D_v f) \cdot g_1(w, u, v, 0), \\ \dot{u} = -\det(D_v f) \cdot g_2(w, u, v, 0), \\ \dot{v} = \text{adj}(D_v f) \cdot ((D_w f) \cdot g_1(w, u, v, \varepsilon) + (D_u f) \cdot g_2(w, u, v, \varepsilon)). \end{cases} \quad (10)$$

where  $\text{adj}(D_v f) \cdot D_v f = D_v f \cdot \text{adj}(D_v f) = \det(D_v f)I$  and  $D_v f$  is a scalar, so  $\text{adj}(D_v f) = 1$ . The condition for a folded singularity is obtained,  $f = 0$ ,  $D_v f = 0$ ,  $D_{vv} f \neq 0$ , and  $D_{w,u} f$  has a full rank of one.

Denote the eigenvalues of desingularized system (10) restricted to the critical manifold as  $\lambda_1, \lambda_2$  and the folded singularity  $\bar{p}$ . According to Definition 4, the folded singularity can be divided into the following categories [66,120]: a folded node, if  $\lambda_1 \cdot \lambda_2 > 0$  and  $\lambda_1, \lambda_2 \in \mathbb{R}$ ; a folded saddle, if  $\lambda_1 \cdot \lambda_2 < 0$  and  $\lambda_1, \lambda_2 \in \mathbb{R}$ ; a folded focus, if  $\lambda_1 \cdot \lambda_2 > 0$  and  $\text{Im}(\lambda_{1,2}) \neq 0$ ; and a folded saddle node, if  $\lambda_1 > 0 = \lambda_2$  or  $\lambda_1 = 0 > \lambda_2$  and  $\lambda_1, \lambda_2 \in \mathbb{R}$ .

Note: a folded saddle node can also be divided into folded saddle nodes of type I and type II. It is called a folded saddle node type I when the folded singularity has a characteristic direction tangent to the folded line  $F$ . In fact, it corresponds to the folded singularity of the saddle-node bifurcation of the folded saddle and folded node pairs. A folded saddle node type II is the eigendirection transversal to the folded line  $F$  of a zero-eigenvalue folded singularity, that is, the folded singularity has a transcritical bifurcation. It is the general singularity from the attracting branch of a critical manifold to the repelling branch by a transcritical bifurcation and vice versa. In fact, it is really the equilibrium point of the whole system, and the other folded singularities are not necessarily projections of the



original system. The corresponding folded singularity at this transcritical bifurcation is the folded saddle node type II. Readers can see the references [12,38] for the detailed analysis of folded saddle nodes.

The canard theorems for some folded singularities are listed below (Theorems 5–8):

**Theorem 5** ([10,12]). *Given fast/slow system (9), for a sufficiently small  $\varepsilon > 0$ , the  $(n - 1)$ -dimensional set  $W_{cs}$  of the singular canard is perturbed to the  $(n - 1)$ -dimensional set of the maximal canard at the folded saddle ( $\lambda_1 < 0 < \lambda_2$ ).*

**Theorem 6** ([10,12,38,66]). *Given fast/slow system (9), for a sufficiently small  $\varepsilon > 0$ , at the folded node ( $\lambda_1 < \lambda_2 < 0$ ), denote  $\mu = \lambda_2/\lambda_1 < 1$ , and the following conclusions are valid:*

- (i) *The perturbation of the  $(n - 1)$ -dimensional set  $W_{ss}$  of the singular strong canard to the  $(n - 1)$ -dimensional set of the largest strong canard is known as the main strong canard;*
- (ii) *If  $1/\mu \in \mathbb{N}$ , the  $(n - 1)$ -dimensional set of the singular weak canard is perturbed to the  $(n - 1)$ -dimensional set of the largest weak canard and called the main weak canard;*
- (iii) *If  $2k + 1 < \mu^{-1} < 2k + 3, k \in \mathbb{N}$  and  $\mu^{-1} \notin 2\mathbb{N} + 2$ , there is a set of  $k$  maximum canards, all  $(n - 1)$ -dimensional, called the secondary canards. The set of  $k$  secondary canards follows a criterion to approximate the main strong canard set in two levels of attraction and repulsion;*
- (iv) *If  $2k + 1 < \mu^{-1} < 2k + 3, k \in \mathbb{N}$  and  $\mu^{-1} \notin 2\mathbb{N} + 2$ , the main strong canard set twists once around the main weak canard set in the  $O(\sqrt{\varepsilon})$  neighbourhood of fold line  $F$ ; meanwhile, the  $j$ th set of the secondary canard,  $1 \leq j \leq k$ , twists  $2j + 1$  times around the main weak canard set in the  $O(\sqrt{\varepsilon})$  neighbourhood of fold line  $F$ ; the twist here is a half-rotation. Each maximal canard set has a different rotation number;*
- (v) *Main weak canards at the folded node have a cross-critical bifurcation, for  $\mu^{-1} \in \mathbb{N}$  and odd, and a tuning-fork bifurcation for even  $\mu^{-1} \in \mathbb{N}$ .*

*The canard structure of the folded node is the key to the small amplitude oscillation occurring in the neuron model by combining the global regression mechanism. It mainly occurs in the fast/slow system with two slow and one fast variables [38,46].*

**Theorem 7.** *In the case of the folded focus [10], all the trajectories starting on the critical manifold's attracting branch eventually arrive at the set of fold points, except the folded singularity within a finite forward or backward time and these trajectories terminate there because of the finite-time explosion; hence, there is no singular canard.*

**Theorem 8** ([12]). *Given fast/slow system (9), for a sufficiently small  $\varepsilon > 0$ , the singular canard corresponding to the nonzero eigenvalues of the linearized part of the desingularized system can always be perturbed to the canard set at the folded saddle node ( $\lambda_1 < 0 = \lambda_2$ ).*

The folded saddle node type II is associated with the global regression mechanism and singular Hopf bifurcation [41,44,120]. Szmolyan and Wechselberger [12,38] used the geometric singular perturbation theory and explosion method to show the strong eigendirection corresponding to the singular canard at the folded node and folded saddle, which could always be perturbed to the maximum canard of the desingularized system. That is, the slow flow of the attracting neighbourhood and repelling neighbourhood of the critical manifold intersected at cross sections. The singular canard of folded saddle node type II could also be perturbed to the maximum canard.

The canard theory can be extended to any  $n > 2$  case. Generally, the set of folded singularities is regarded as the sum of the equilibrium sets of the desingularized system, which has  $(n - 2)$  zero eigenvalues and two eigenvalues with nonzero real parts. The set of folded singularities represents the normally hyperbolic manifold of the equilibrium point of the desingularized system. The types of folded singularities are determined by the two nonzero eigenvalues, which can be divided into folded node, folded saddle, and folded focus. In the case where  $m > 1$  and  $n = 2$ , the fold line of the system is required to have only one zero eigenvalue in the  $m$ th-order linearized matrix of the fast equation. In this way,

the local centre manifold can be expressed in terms of slow variables and one-dimensional fast variables. The  $m > 1$  system is discussed in the literature [66]. The canard is further discussed in the following.

### 3.3. Torus Canards

Consider the fast/slow system on the two-torus [14] (11):

$$\begin{cases} \dot{x} = f(x, y, \varepsilon), \\ \dot{y} = \varepsilon g(x, y, \varepsilon), \end{cases} \quad (x, y) \in T^2 \cong \mathbb{R}^2 / (2\pi\mathbb{Z}^2), \varepsilon \in (\mathbb{R}, 0). \quad (11)$$

Here,  $f, g$  are perfectly smooth. Denote  $M := \{(x, y) | f(x, y, 0) = 0\}$ . Assume that the local generics of the system satisfy the following conditions:

- (C1) The speed of slow flow is bounded away from zero:  $g > 0$ ;
- (C2)  $M$  is a smooth curve;
- (C3) The lift of curve  $M$  to the covering coordinate plane is contained within the fundamental square  $\{|x| < \pi, |y| < \pi\}$  and is convex, meaning, in particular, that there are two jump points (straight and inverse jumps), the two points on the far right and the far left of  $M$ ; we denote them as  $G^-$  and  $G^+$ , respectively;
- (C4) For any point  $(x, y) \in M \setminus \{G^+, G^-\}$ , the following nondegenerate assumption holds:

$$\frac{\partial f(x, y, 0)}{\partial x} \neq 0;$$

- (C5) The nondegenerate assumption at the jump point is valid:

$$\frac{\partial^2 f(x, y, 0)}{\partial x^2} \Big|_{G^\pm} \neq 0, \quad \frac{\partial f(x, y, 0)}{\partial y} \Big|_{G^\pm} \neq 0.$$

C1–C5 define an open set in the space of fast/slow systems on a two-torus.

**Theorem 9** ([13–15,47]). *Given system (11) satisfying the above five conditions, there is one disjoint interval sequence  $\{R_n\} = [\alpha_n, \beta_n]$  and two disjoint interval sequences  $C_n^\pm \subset R_n$ , and the following property is true:*

- (i) For some  $C > 0$ ,  $|R_n| = O(e^{-Cn})$ .
- (ii)  $\alpha_n = O(1/n)$ .
- (iii) For every  $\varepsilon$  sufficiently small, not belonging to any  $R_n$ , the rotation number  $\rho(\varepsilon)$  is an integer. The system has exactly two hyperbolic periodic trajectories, one stable and one unstable, and the unstable one contains canards.
- (iv) For every sufficiently small  $\varepsilon \in C_n^\pm$ , the system has exactly two periodic trajectories, both of which are a hyperbolic torus canard, and one is stable and the other is unstable.

The above theorem gives the relevant theoretical explanation for the existence and uniqueness of the torus canard of the two-dimensional plane. Of course, the existence of the torus canard has also been found for high-dimensional nonlinear fast/slow systems [48–51,53,54]. It is known that the necessary condition for a torus canard is the existence of attracting and repelling limit cycles, that is, a saddle-node limit cycle accompanied by a torus bifurcation, which is very similar to the limit-cycle canard, which is a saddle node accompanied by a Hopf bifurcation, that is, the fixed point of attraction and repulsion. Thus, one is the canard along the equilibrium point and the other is the canard around the saddle-node limit cycle. Of course, in addition to the Hopf canard, canard phenomena have been shown near the folded node, folded saddle, and folded saddle node mentioned above. Some researchers found mixed types of canards in neuron models, that is, the limit-cycle canard and the torus canard appeared simultaneously in the model [50]. Such canard phenomena may occur near the Bogdanov–Takens point and exhibit a subcritical Hopf bifurcation.

#### 4. Canards and the Discharge Rhythm of Neuron Model

##### 4.1. Limit-Cycle Canards and MMOs of Neuron Model

Assume canonical system (12) [120]:

$$\begin{cases} \varepsilon x' = y - x^2 - x^3, \\ y' = z - x, \\ z' = -v - ax - by - cz. \end{cases} \quad (12)$$

The critical manifold of this system is an S-shaped surface, which makes it possible for the trajectories to leave the neighbourhood of the origin and return. Figures 1–4 in reference [127] show the MMOs caused by a Hopf bifurcation under specific parameter settings. Two fold curves  $x = 0$  and  $x = -\frac{2}{3}$  divide the critical manifold into two sections of attracting branch surfaces and one section of a repelling branch surface. Under this set of parameters, there is a saddle-focus point,  $p$ , on the repelling branching surface near the origin of the system (the folded node). It has a pair of unstable complex eigenvalues, where the singular Hopf bifurcation occurs. The trajectory of the system starts from the intersection of point  $p$  and is restricted by the two-dimensional unstable manifold. The trajectory spirals away from  $p$  while repeatedly intersecting with the repelling branching surface (small amplitude oscillations). Finally, it crosses through the repelling branch surface of the middle branch and jumps to the attracting branch  $x < -\frac{2}{3}$ . Meanwhile it reaches the fold line  $x = -\frac{2}{3}$ , due to being constrained by the slow flow of the attracting branch, and jumps again to the attracting branch  $x > 0$ . The trajectory returns to the fold line  $x = 0$  again and finally returns to the saddle focus  $p$  under the constraints of a slow flow and a one-dimensional stable manifold. This period trajectory is repeated and the MMOs form. It is much more difficult to find the limit-cycle canard in high-dimensional nonlinear neuron models than in simple neuron models. Because of their high sensitivity to parameters, it is not easy to determine the influencing factors in complex parameter systems. Therefore, it is still necessary to explore more effective methods and approaches for the study of the high-dimensional limit-cycle canard.

##### 4.2. Folded-Saddle Canards, Firing-Threshold Manifold, and Parabolic Bursters of Neuron Model

This model is presented as a classical conductance-based parabolic burster, which is shown in Equation (2) in reference [39]. Figure 3 in the reference describes the transformation of the transitive slow-wave solution to the periodic burster (for both sets of parameters). The stable slow-wave solution  $\Gamma_{sw}$  (Figure 3a1) is fully included in the stable manifold neighbourhood (Figure 3b1), also in the singular true canard. To transition the phase of the burster to the resting state, it is necessary to pass through the lower saddle-node invariant loop curve  $F^+$  (Figure 3a2), which is the characteristic of the parabolic burster. Except for the trajectory of the canard fragment (the beginning of the spike-adding), the parabolic burster trajectory starts and ends its flow into the fold line  $F^+$ 's neighbourhood. For the fixed neighbourhood of the attracting critical manifold and repelling critical manifold, there exists a unique singular true canard from the neighbourhood of the attracting critical manifold to the neighbourhood of the repelling critical manifold connecting the neighbourhood of the folded saddle [12]. The singular faux canard and the singular true canard are separated by the folded homoclinic bifurcation. The transition from resting to burster state is as the periodic orbit of the stable slow-wave solution. When it continues to approach the singular true canards, beginning to form the canard's segment, it eventually contains the largest canard's segment and returns to the down-attracting critical manifold neighbourhood by jumping off the upper fold line (Figure 4a in reference [39]). The dynamic properties near the folded saddle in the attracting neighbourhood of the critical manifold are close to the dynamics of the saddle, which means that the flow has strong compression properties. In other words, all the trajectories close to the folded saddle on the attracting critical manifold can be attracted together in a sufficiently long time. It forms a thin tube, which approaches the singular faux canard with an  $O(\varepsilon)$  velocity. The regular burster satis-

fies the condition that all trajectories in the tube reach the jump point on the fold line (the opposite of the singular true canard) and the dynamics of the fast fibre follow. The trajectory follows the dynamics of the saddle-node invariant loop back near the fold line and re-enters the compressed tube through the fold line with an  $O(\varepsilon^{2/3})$  velocity, meaning it re-enters the resting state. The trajectory in the tube repeats this process over and over again. Finally, the trajectory of the return tube follows the saddle-node invariant loop connected to the singular true canard (Figure 4b–d in reference [39]). If it is assumed that the singular faux canard can exist by modifying the neighbourhood of the attracting critical manifold and that the thin tube is its canard centre, then the thin tube will attract the dynamics from the fold line. In a sense, the mechanism of transferring the periodic orbital of the slow-wave solution to the burster may be described as a connection between the singular faux canard and the singular true canard, where the attractor is the periodic burster itself, rather than the previous periodic orbital. Thus, the folded saddle-node canard principle may explain the parabolic burster mechanism of the neuron model.

The firing threshold manifold of excitatory neurons is also closely related to the canard of the folded saddle type [6], which gives the case of the single threshold of bound firing. Of course, some researchers used the combination mechanism of the folded-saddle canard and the folded-node canard to illustrate the generation mechanism of square-wave bursters [128]. The folded-saddle canard can explain the increased large-amplitude oscillation in each burster, and the folded node canard can explain the control mechanism of small-amplitude oscillations in each burster. At present, the interpretation of the burster pattern by the folded-saddle canard with a high-dimensional nonlinear model needs to be strengthened, because of the tedious computational complexity of the high-dimension model. The study on the firing mode of neurons should be continuously improved, because of the complex dynamic behaviour caused by the stability and instability manifolds of the folded-saddle canard. Perhaps it provides a more effective way to explain the transition in neuron firing patterns.

#### 4.3. Folded-Node Canards and MMOs in Neuron Model

In the first section, we gave some conceptual definitions of singular systems, such as the reduced problem, layer problem, Fenichel theory, critical manifold, fold line, folded singularity, and so on. This section illustrates the connection between the folded-node canard theory and MMOs for the actual lactotroph neuron model. This section introduces a simplified three-dimensional model (13):

$$\begin{cases} C_m \frac{dV}{dt} = -(I_{Ca} + I_K + I_{SK} + I_{BK} + I_A), \\ \tau_n \frac{dn}{dt} = \lambda(n_\infty(V) - n), \\ \frac{d[Ca]}{dt} = -f_c(\alpha I_{Ca} + k_c[Ca]). \end{cases} \quad (13)$$

After processing, the system is transformed into the standard form of singular perturbation system (14), and the reduced problem and layer problem of the system are obtained accordingly. The dynamic behaviour of the whole system is discussed by combining the two problems. The decomposition process is no longer given here, and a detailed analysis is shown in reference [123]. System (14) is as follows:

$$\begin{cases} \varepsilon \frac{dv}{d\tau} = -(\bar{I}_{Ca} + \bar{I}_K + \bar{I}_{SK} + \bar{I}_{BK} + \bar{I}_A) \triangleq f(v, n, [Ca]), \\ \frac{dn}{d\tau} = \lambda(n_\infty(v) - n) / \tau_n \triangleq g_1(v, n), \\ \frac{d[Ca]}{d\tau} = -f_c(\alpha \bar{I}_{Ca} + k_c[Ca]) \triangleq g_2(v, [Ca]). \end{cases} \quad (14)$$

**Statement 1** ([66,123]). *The critical manifold  $S_0$  of singular perturbation system (14) is a locally folded surface.*

From the definition of critical manifolds, the actual graph surface of a local critical manifold is shown in Figure 1 in reference [123]. We can show that  $f$  and  $f_v$  (partial derivatives of  $f(v, n, [Ca])$  to  $v$ ) are continuous bounded functions in the closed regions  $I = [-80, 10] \times [0, 0.3] \times [0.2, 0.4]$ . By the intermediate value theorem on continuous functions, we know that the null surface  $f_v$  exists. Therefore, Figure 1b shows the fold line intersected by  $f$  and  $f_v$ . The surface diagram of locally critical manifold  $S$  is given in Figure 1a, where  $S = \{(v, n, [Ca]) \in I, f(v, n, [Ca]) = 0\}$  and  $S = S_a^+ \cup L^+ \cup S_r \cup L^- \cup S_a^-$ .  $S_a^\pm = \{(v, n, [Ca]) \in S, f_v(v, n, [Ca]) < 0\}$  are two attracting branches and  $S_r = \{(v, n, [Ca]) \in S, f_v(v, n, [Ca]) > 0\}$  is a repelling branch.  $L^\pm = \{(v, n, [Ca]) \in S, f_v(v, n, [Ca]) = 0, f_{vv}(v, n, [Ca]) \neq 0\}$  are two folded curves.  $\Gamma_1$  is the trajectory phase diagram of the whole system, which well explains the dynamic transition of the system. Following the trajectory arrow, the system trajectory remains in the lower resting state until it reaches the fold curve  $L^-$  along the slow flow of the lower attracting branch. It quickly transitions along the fast fibre to the upper attracting branch and follows the slow flow of the upper attracting branch to the fold curve  $L^+$ . Finally, it returns to the resting state of the lower attracting branch along the other fast fibre and passes the jump point on  $L^+$ .

**Statement 2** ([66,123]). There exists a folded singular node  $P_0 \in L^\pm$  in singular perturbation system (14), which satisfies  $f_n g_1 + f_{[Ca]} g_2 = 0$ , and the eigenvalues of the Jacobian matrix of the reduced system restricted to  $S$  at  $P_0$  are  $-9209836.318$  and  $-0.1598397647$ .

Figure 2 in reference [123] shows the system trajectory and fold curve as well as the projection near the folded singularity  $P_0$ . The folded singularities of the system satisfy:

$$f(P_0) = 0, \frac{\partial f}{\partial v}(P_0) = 0, \frac{\partial^2 f}{\partial v^2}(P_0) \neq 0, \frac{\partial f}{\partial n}(P_0)g_1(P_0) + \frac{\partial f}{\partial [Ca]}(P_0)g_2(P_0) = 0.$$

Then, the type of singularity is determined according to the eigenvalue of the desingularized system in  $P_0$ , which is obtained by the reduction system of the whole system. However, the canard of the folded singularity can always be perturbed to the maximum canard.

**Statement 3** ([66,123]). There exists a periodic orbit  $\Gamma = \Gamma_a \cup \Gamma_g$  for singular perturbation system (14), the smooth segment  $\Gamma_a$  is the trajectory that is in the interior of the singular funnel with  $P_0$  as the ending point, and  $\Gamma_g = \Gamma_a^+ \cup \Gamma_f^+ \cup \Gamma_a^- \cup \Gamma_f^-$ , where  $\Gamma_a^\pm$  is the orbit to connect  $L^\pm$  and  $P(L^\mp)$ , and  $\Gamma_f^\pm$  is the fast fibres to connect  $L^\pm$  and  $P(L^\pm)$ . (Note:  $P(L^\pm)$  is the trajectory which is projected by  $L^\pm$  along the direction of the fast fibres to the lower (upper) attracting branch of the critical manifold.)

In the second part, we know that  $P_0$  is a folded node, so there is a maximum canard (strong canard). The shaded part near point  $P_0$  in Figure 2a [123] represents the singular funnel, which is enclosed by the strong canard direction  $SV$  and the fold curve  $L^+$ . For the small amplitude oscillation  $\Gamma_1$  in the funnel, we expect a singular trajectory connection between the small amplitude oscillation and the relaxation oscillation outside. By theorem [10,66,68], we have an assumption that there exists a subset  $N^\pm \subset P(L^\mp)$  with the characteristic that it can arrive at the folded curve  $L^\pm$  when all trajectories of the slow subsystem satisfy the initial domains in  $N^\pm$ . Thus, the associated maps can be defined by  $\Pi^\pm : N^\pm \subset P(L^\mp) \mapsto L^\pm$ . Moreover, the return map can be defined by  $\Pi \triangleq P \circ \Pi^+ \circ P \circ \Pi^- : N^- \mapsto P(L^+)$ , and  $\Pi(N^-) \subset N^-$ . According to the contracted mapping principle and Brouwer's fixed point theorem, we can prove the existence of a singular periodic orbit. By the return map, small amplitude oscillations can return to the singular funnel, while MMOs emerge. We can obtain the following conclusion:



**Theorem 10** ([66,123]). Suppose that all assumptions in Statement 1–3 are established, then, for a sufficiently small  $\varepsilon$ , there exists a stable MMOs of type  $1^s$  for singular perturbation system (14), for certain determined  $s > 0$ .

Note: If segment  $\Gamma_a$  of singular periodic trajectory  $\Gamma$  consists of the boundary segment of the singular funnel (the strong canard), then there are more complex MMO types  $L^{s'}$ , and  $L \geq 1$  and  $s' \leq s$  are all possible. Moreover, this theorem can only explain the MMOs of the system trajectory entering the singular funnel but cannot explain the MMOs falling outside the funnel, that is, it is sufficient but not necessary.

In fact, the folded-node canard has been explained in the most detail and there are specific theories about its relationship with partial MMOs, but there are still unexplained, mixed discharge modes. We also use this theory to describe the existence of  $1^s$ -type MMOs, but for more complex high-dimensional nonlinear systems, relevant improvements need to be made or more reasonable methods need to be sought to explain the discharge modes. The research on the  $L^{s'}$  pattern still needs a more specific theoretical explanation and the exploration on the mixing pattern of neurons is still continuing.

#### 4.4. Torus Canards and Transition between Spiking and Bursting

The torus canard in neurons was first observed in the cerebellar Purkinje cell model [48], which explained the torus canard transition dynamics between tonic spiking and bursting in a simplified five-dimensional model. Later, in some familiar classical neuron models such as Hindmarsh–Rose, Morris–Lecar, and Wilson–Cowan models, different firing types of the torus canard were found. Canard types were, respectively, sub-Hopf/fold cycle, circle/fold circle, and fold/fold circle [51]. At the same time, it was also proposed that there may be other types of torus canards in the neuron model, such as sup-Hopf/fold circle [92] and top-hat burster [129]. The dynamic behaviour of the mixed limit-cycle canard and the torus canard has also been found in the improved Wilson–Cowan–Izhikevich model [50]. At the same time, the torus canard behaviour in the neuron model has been continuously favoured by researchers and deeply discussed and is well understood [53]. In this section, the five-dimensional model of the cerebellar Purkinje cell is used to illustrate the main process of the changes of the torus canard. The five-dimensional model of the cerebellar Purkinje cell [48] as follows (15):

$$\begin{cases} \dot{V} = -J - g_K n^4 (V + 95) - g_{Na} m_0^3 (V) h (V - 50) \\ -g_L (V + 70) - g_{Ca} c^2 (V - 125) - g_M M (V + 95), \\ \dot{x} = (x_0(V) - x) / \tau_x(V). \end{cases} \quad (15)$$

where  $x$  represents  $n, h, c$ , and  $M$ .

As the external parameter  $J$  decreases, we describe the membrane voltage transition process. Considering Figure 2 in reference [48], firstly, the membrane voltage shows a strict burster pattern at  $J = -23$ , the burster interval (the duration from the end of the last spike of a burster to the beginning of the next burster) is displayed as 100 ms, and the burster duration (the time interval between the beginning of the first spike and the end of the last spike of the burster) is significantly smaller than the burster interval. With  $J$  decreasing to  $-32.9380$ , the burster time increases gradually, and the burster time is longer than the interval time. If parameters are slightly changed, the burster appears with a modulated amplitude, which is also the beginning of the transition from burster to single-spiking mode. When  $J$  decreases to  $-33.0$ , the membrane potential completely shows an amplitude modulation discharge. Finally, when  $J = -33.0$ , the membrane potential presents a single-spiking mode, which realizes the transition from the burster to the single-spiking mode through an amplitude modulation. The corresponding dynamic analysis is shown in Figure 4 in reference [48]. When the membrane potential is completely in the burster mode, the discharge transition of the system starts from the fold point of the fast subsystem. The whole system dynamics quickly transitions to the attracting limit cycle and finally

reaches the saddle-node limit cycle. The dynamics transitions to the resting state and the system shows a fold/fold-circle burster mode. With the decrease in  $J$ , the dynamics of the whole system at  $J = -32.93825$  is accompanied by the repelling limit cycle through the saddle-node limit cycle and finally transition to the stable limit cycle or the stable fixed point of the lower branch, which may be called the canard with a head. When  $J = -32.94$ , the discharge rhythm of the model is only presented as amplitude-modulated spiking. The dynamics follow the attracting limit cycle to the saddle-node limit cycle. Then, as  $M$  decreases, it temporarily follows the repelling limit cycle before returning to the attracting branch, which may be called the canard without a head. In the case of a single-spiking discharge, the single period corresponds to the stable single-spiking mode, reducing the membrane potential to maintain the dynamics of the single limit cycle until the system shows no discharge state.

Canards have also been found in other mathematical models of neural systems [31,68]. However, these canards appear along the attracting and repelling branches of the fixed point. The canards' dynamics presented here appear along the attracting and repelling branches of the limit cycle in a real biophysical model. By studying the canard mechanism of a reduced five-dimensional model of the cerebellar Purkinje cell, we obtained a better understanding of its physiological mechanism (the M-current). Similar results also occur in a detailed biophysical model. Clearly, this canard process requires a bifurcation of the stable torus and the emergence of stable and unstable limit cycles (i.e., tori's bifurcation and saddle node of limit cycle). The Poincare map apparently gives the most direct statement of the existence of the limit cycle and torus canard. In fact, the torus canard is a combination of numerical simulation and mathematical theory in order to explain the transition from spiking to burster mode, which provides a new way to explain the transition from the spiking mode. Perhaps due to the extreme sensitivity of some parameters of mathematical properties, some discharge patterns cannot be explained theoretically, and a numerical simulation can be first combined with a mathematical theory to elaborate. The torus canard is relatively effective for the interpretation of high-dimensional neuron burster patterns because of the combination of numerical results and theoretical explanations.

#### 4.5. "Blue Sky Catastrophe" and Transition between Spiking and Bursting

Shilnikov et al. first expounded three cases of "blue sky catastrophe" in singular perturbed systems and their strict proof [130]. Then, the transition between single-spiking and burster modes was explained for the simplified three-dimensional cardiac interneuron cell model of the leech [55]. The homoclinic bifurcation of the associated periodic orbit was used to explain the transition process between single-spiking and burster modes [52,131–135]. In this section, the "blue sky catastrophe" is used to elaborate the transition between single-spiking and burster modes. The simplified three-dimensional leech model of the heart interneuron is as follows (16):

$$\begin{cases} CV' = -[\bar{g}_{K_2} m_{K_2}^2 (V - E_K) + g_l (V - E_l)] \\ \quad + \bar{g}_{Na} h_{Na} (V - E_{Na}) f(-150, 0.0305, V)^3 + I_{pol}, \\ m'_{K_2} = [f(-83, 0.018 + V_{K_2}^s, V) - m_{K_2}] / \tau_{K_2}, \\ h'_{Na} = [f(500, 0.0325, V) - h_{Na}] / \tau_{Na}. \end{cases} \quad (16)$$

Here, only the process of the burster mode transition to the single-spiking mode is described and the definition of average voltage and average nullcline is not detailed. From Figure 2 in reference [55], the membrane voltage gradually transits from the burster mode to the single-spiking mode (the fourth line) as the control bifurcation variable  $V_{K_2}^s$  decreases to  $-24.8$ . Moreover, the fifth line is the specific amplification of the membrane voltage. The saddle-node periodic orbit  $L_{bs}$  (each intersection point of average voltage and average nullcline corresponds to a periodic orbit [136]) is the first component of the "blue sky catastrophe" of the fast/slow system, which divides the system into two unique manifolds. The strong stable manifold divides the trajectory near the saddle-node periodic orbit into

two parts: a node region and a saddle region. The node region attracts the trajectory to the periodic orbit and the saddle region repels the trajectory to the periodic orbit. The unstable manifold is attracted to the saddle-node periodic orbit in backward time. In other words, the phase point of the right trajectory of the saddle-node periodic orbit moves to the left along the lower branch of the repolarization equilibrium point (the position of the saddle node is lower than the position of the saddle-node periodic orbit) following the management of the burster mode and finally returns to the saddle-node periodic orbit from the left. Therefore, the global instability manifold's homoclinic joins the periodic trajectory, which is the second part of the "blue sky catastrophe". The average nullcline  $\langle m'_{k_2} \rangle = 0$  is restricted by the control bifurcation parameter. Assuming that the bifurcation parameter  $V_{k_2}^s$  is greater than the critical value, the periodic orbit of the saddle node will decouple into a stable node and an unstable saddle. Stable nodes correspond to the single spiking mode of neurons, and the latter may correspond to the burster mode state, which involves the coexistence of single-spiking and burster modes. When the bifurcation parameter is less than the critical value, the saddle-node periodic orbit disappears and generates a new stable large-amplitude and large-period periodic trajectory (Figure 1 in reference [55]). This trajectory corresponds to the burster mode of neurons, consisting of a resting state and a burster state, where the burst duration is estimated through  $1/\sqrt{V_{k_2}^s - 24.25}$ , since the phase points need to pass through the phantom saddle node. Therefore, by controlling the distance between the bifurcation parameter and the critical value, the burst duration can be controlled. This process of changing the single parameter variation realizes the continuous transition from burster mode to single-spiking mode through the "blue sky catastrophe" bifurcation, and it is reversible. By determining that the standard deviation of the period of the burster oscillation is equal to zero, the system presents as a stable periodic orbit. This is a typical case of using the shape of the burster pattern combined with mathematical theory to explain the theoretical process of firing transition. It involves the average field of the fast/slow variables and suggests that we may also use other mathematical methods to explain the transitions between spiking and spiking, burst and burst, spiking and burst. This will be very useful for our understanding of the effects of neuronal feedback control. It is worth considering using the shape of the burster pattern combined with mathematical theory to explain the rhythm dynamics of the neuron.

## 5. Summary and Outlook

In this paper, the existence of canards in neuron models was explored. The relationship between the folded-node canard and MMOs was analysed. The link between a singular Hopf bifurcation and MMOs has been discussed in special models but rarely in the analysis of neuron models. The association between folded saddle and parabolic bursters was also found in the improved neuron model. The transition relationship between single-spiking and burster modes is very common in higher-dimension models. Here, we also covered the transition between single-spiking and burster modes using the idea of the "blue sky catastrophe". Moreover, recently related studies have appeared, which may provide a new way to explain transition dynamics [137]. The novelty of this work lies in the theoretical explanation of the rhythmic firing of the neuron models. The transient transition mechanism of the neuron models was explained, which may be more interesting than the rhythmic firing itself. Canards can formulate these phenomena well. These are very helpful for understanding the dynamics and biological mechanisms of biophysical models. Furthermore, these theoretical results were well explained by the calculated graphs.

The core focus of this paper was to explain the rhythm dynamics of the neuron model based on the canard mechanism, by mainly expounding the relationship between the limit-cycle canard, the folded-singularity canard, the torus canard, and the rhythm discharge of neuron. There are still many problems that need to be improved and solved in these studies. The detection of the three-dimensional singular Hopf canard mechanism and its relationship with the discharge mode of the neuron model are still lacking the corresponding research of whether the folded node in the three-dimensional neuron model

can also find the mixing-mode mechanism other than type 1<sup>s</sup>, or find a more reasonable method to explain the more complex mixing oscillation mode. The relationship between folded saddle and neuron firing mode still needs further explanation, because it always has a one-dimensional stable manifold and a one-dimensional unstable manifold, which makes the properties of the system more complex. The singular canard of high-dimensional (greater than three) neuron models and the discharge mechanism of the neuron are still difficult problems. It is urgent to explore the relationship between the neuron rhythm transition and the torus canard. The high nonlinearity characteristic of the neuron model is a major confusion in the implementation of model dynamics' analysis. The method of singular perturbation system mentioned in this paper is actually a processing method of dimension reduction analysis. Of course, other reasonable dimensionality reduction methods can be found to explain the discharge mode of high-dimensional models, such as the dimensionality reduction of the system by the centre manifold theorem, the Lyapunov–Schmidt method, Galerkin method commonly used in engineering, etc. [138]. Applying these methods to neuron models is something we will consider in the future. It is hoped that the network dynamics can be explained in detail through the firing mode of the output end of the neuron network. These results are better to feedback the dynamic properties of the control network model. The physiological mechanism may be better understood by exploring the dynamics of a realistic physiological model. The ultimate attribution of all computational neural networks may still come from biological neural networks, or it may come through nerve impulses to pinpoint the nature of the network.

In view of these phenomena, some theoretical methods give a partial explanation, but the extension to high-dimensional results and the specific implementation process may not be able to achieve the ideal effect. Therefore, with a concrete implementation process, some reasonable methods may be found to solve it. Of course, these analyses are limited to the neuron model with a canard behaviour. We may also combine additional mathematical research methods to explain the discharge mode and transition dynamics of the neuron model, such as the fast/slow dynamic method, etc. In future research, our focus will have two parts. One is the transient transition between neuronal rhythm firing (transition between spiking, between spiking and bursting, between bursting and bursting). The physiological information of transient transition may be no less than that of the rhythm discharge itself. The other is a passion for the dimensionality reduction of high-dimensional biophysical models. Dimensionality reduction and preserving the physiological mechanism as much as possible is what we would like to achieve. The above research will be helpful to understand the dynamics and physiological mechanism of biophysical models. It is hoped that these studies can provide a priori theoretical support for experimental neuroscience.

**Author Contributions:** Conceptualization, F.Z. and S.L.; methodology, F.Z.; software, F.Z.; validation, F.Z.; formal analysis, J.S. and Y.Z.; investigation, F.Z.; writing—original draft preparation, F.Z.; writing—review and editing, F.Z., J.S. and Y.Z.; supervision, S.L. All authors have read and agreed to the published version of the manuscript.

**Funding:** This work was funded by the National Natural Science Foundation of China (grant no. 12202208 and 11872183), the Basic Science (Natural Science) Research Project of Colleges and Universities of Jiangsu Province (grant no. 22KJB130009, no. 22KJB310019), the Research and Cultivation Project for Young Teachers of Nanjing Audit University (grant no. 2021QNPY015), The Scientific Research Foundation of high-level personnel of Taizhou University (grant no. TZXY2021QDJJ001), 2022 Doctoral program of Entrepreneurship and Innovation in Jiangsu Province, “2022 Taizhou Tuo Ju Project” for Young science and Technology Talents, the Project of Excellent Science and Technology Innovation Team of Taizhou University, the China Scholarship Council (grant no. 202206150096).

**Data Availability Statement:** The data presented in this study are available on request from the corresponding author.

**Conflicts of Interest:** The authors declare no conflict of interest.

## Abbreviations

The following abbreviations are used in this manuscript:

MMOs    Mixed-mode oscillations

## References

- Diener, F.; Diener, M. Chasse au canard. I. Les canards. *Collect. Math.* **1981**, *1*, 37–74.
- Diener, M. The canard unchained or how fast/slow dynamical systems bifurcate. *Math. Intell.* **1984**, *6*, 38–49. [[CrossRef](#)]
- Diener, M. Regularizing microscopes and rivers. *SIAM J. Math. Anal.* **1994**, *25*, 148–173. [[CrossRef](#)]
- Desroches, M.; Guillemon, A.; Ponce, E.; Prohens, R.; Rodrigues, S.; Teruel, A.E. Canards, folded nodes and mixed-mode oscillations in piecewise-linear slow-fast systems. *SIAM Rev.* **2016**, *58*, 653–691. [[CrossRef](#)]
- Harvey, E.; Kirk, V.; Osinga, H.M.; Sneyd, J.; Wechselberger, M. Understanding anomalous delays in a model of intracellular calcium dynamics. *Chaos* **2010**, *20*, 045104. [[CrossRef](#)]
- Mitry, J.; McCarthy, M.; Kopell, N.; Wechselberger, M. Excitable neurons, firing threshold manifolds and canards. *J. Math. Neurosci.* **2013**, *3*, 12. [[CrossRef](#)]
- Wieczorek, S.; Ashwin, P.; Luke, C.M.; Cox, P.M. Excitability in ramped systems: The compost-bomb instability. *Proc. R. Soc. Math. Phys. Eng. Sci.* **2011**, *467*, 1243–1269.
- McCarthy, M.; Kopell, N. The effect of propofol anesthesia on rebound spiking. *SIAM J. Appl. Dyn. Syst.* **2012**, *11*, 1674–1697. [[CrossRef](#)]
- Wechselberger, M.; Mitry, J.; Rinzel, J. Canard theory and excitability. In *Nonautonomous Dynamical Systems in the Life Sciences*; Kloeden, P.E., Pötzsche, C., Eds.; Springer: Cham, Switzerland, 2013; pp. 89–132.
- Wechselberger, M. À propos de canards (Apropos canards). *Trans. Am. Math. Soc.* **2012**, *364*, 3289–3309. [[CrossRef](#)]
- Benoit, E. Chasse au canard. *Collect. Math.* **1981**, *32*, 37–119.
- Szmolyan, P.; Wechselberger, M. Canards in  $R^3$ . *J. Differ. Equ.* **2001**, *177*, 419–453. [[CrossRef](#)]
- Guckenheimer, J.; Ilyashenko, Y. The duck and the devil: Canards on the staircase. *Mosc. Math. J.* **2002**, *1*, 27–47. [[CrossRef](#)]
- Schurov, I.V. Ducks on the torus: Existence and uniqueness. *J. Dyn. Control Syst.* **2010**, *16*, 267–300. [[CrossRef](#)]
- Schurov, I.; Solodovnikov, N. Duck factory on the two-torus: Multiple canard cycles without geometric constraints. *J. Dyn. Control Syst.* **2016**, *23*, 481–498. [[CrossRef](#)]
- Benoit, E. Systemes lents-rapides dans  $R^3$  et leurs canards. *Société Mathématique de France Astérisque* **1983**, *109–110*, 159–191.
- Eckhaus, W. Relaxation oscillations including a standard chase on French ducks. In *Asymptotic Analysis II*; Verhulst, F., Ed.; Springer: Berlin, Germany, 1983; pp. 449–494.
- Mishchenko, E.F.; Rozov, N.K. Differential equations with small parameters and relaxation oscillations. In *Mathematical Concepts and Methods in Science and Engineering*; Springer: Boston, MA, USA, 1980.
- Dumortier, F.; Roussarie, R. *Canard Cycles and Center Manifolds*; American Mathematical Society: Providence, RI, USA, 1996.
- Krupa, M.; Szmolyan, P. Relaxation oscillation and canard explosion. *J. Differ. Equ.* **2001**, *174*, 312–368. [[CrossRef](#)]
- Szmolyan, P.; Wechselberger, M. Relaxation oscillations in  $R^3$ . *J. Differ. Equ.* **2004**, *200*, 69–104. [[CrossRef](#)]
- Dumortier, F. Techniques in the theory of local bifurcations: Blow-up, normal forms, nilpotent bifurcations, singular perturbations. In *Bifurcations and Periodic Orbits of Vector Fields*; Schlomiuk, D., Ed.; Springer: Dordrecht, The Netherlands, 1993; pp. 19–73.
- Dumortier, F. Local study of planar vector fields: Singularities and their unfoldings. *Stud. Math. Phys.* **1991**, *2*, 161–241.
- Krupa, M.; Szmolyan, P. Geometric analysis of the singularly perturbed planar fold. In *Multiple-Time-Scale Dynamical Systems*; Jones, C.K.R.T., Khibnik, A.I., Eds.; Springer: New York, NY, USA, 2001.
- Krupa, M.; Szmolyan, P. Extending slow manifolds near transcritical and pitchfork singularities. *Nonlinearity* **2001**, *14*, 1473. [[CrossRef](#)]
- Krupa, M.; Szmolyan, P. Extending geometric singular perturbation theory to nonhyperbolic points—Fold and canard points in two dimensions. *SIAM J. Math. Anal.* **2001**, *33*, 286–314. [[CrossRef](#)]
- Christopher, K.R.T.J. Geometric singular perturbation theory. In *Dynamical Systems*; Johnson, R., Ed.; Springer: Berlin/Heidelberg, Germany, 1995; pp. 44–118.
- Kaper, T.J. An introduction to geometric methods and dynamical systems theory for singular perturbation problems. *Proc. Symp. Appl. Math.* **1999**, *56*, 85–131.
- Robert, E.O.M.J. *Singular Perturbation Methods for Ordinary Differential Equations*; Springer: New York, NY, USA, 1991.
- Fenichel, N. Geometric singular perturbation theory for ordinary differential equations. *J. Differ. Equ.* **1979**, *31*, 53–98. [[CrossRef](#)]
- Guckenheimer, J.; Hoffman, K.; Weckesser, W. Numerical computation of canards. *Int. J. Bifurcat. Chaos* **2000**, *10*, 2669–2687. [[CrossRef](#)]
- Desroches, M.; Krauskopf, B.; Osinga, H.M. Numerical continuation of canard orbits in slow-fast dynamical systems. *Nonlinearity* **2010**, *23*, 739–765. [[CrossRef](#)]
- Vo, T.; Bertram, R.; Wechselberger, M. Bifurcations of canard-induced mixed mode oscillations in a pituitary Lactotroph model. *Discret. Contin. Dyn. Syst.* **2012**, *32*, 2879–2912. [[CrossRef](#)]
- Rotstein, H.G.; Wechselberger, M.; Kopell, N. Canard induced mixed-mode oscillations in a medial entorhinal cortex layer II stellate cell model. *SIAM J. Appl. Dyn. Syst.* **2008**, *7*, 1582–1611. [[CrossRef](#)]



35. Wechselberger, M.; Weckesser, W. Homoclinic clusters and chaos associated with a folded node in a stellate cell model. *Discret. Contin. Dyn. Syst.* **2009**, *2*, 829–850. [\[CrossRef\]](#)
36. Desroches, M.; Krauskopf, B.; Osinga, H.M. The geometry of slow manifolds near a folded node. *SIAM J. Appl. Dyn. Syst.* **2008**, *7*, 1131–1162. [\[CrossRef\]](#)
37. Guckenheimer, J.; Haiduc, R. Canards at folded nodes. *Mosc. Math. J.* **2005**, *5*, 91–103. [\[CrossRef\]](#)
38. Wechselberger, M. Existence and bifurcation of canards in  $R^3$  in the case of a folded node. *SIAM J. Appl. Dyn. Syst.* **2005**, *4*, 101–139. [\[CrossRef\]](#)
39. Desroches, M.; Krupa, M.; Rodrigues, S. Spike-adding in parabolic bursters: The role of folded-saddle canards. *Phys. D* **2016**, *331*, 58–70. [\[CrossRef\]](#)
40. Mitry, J.; Wechselberger, M. Folded saddles and faux canards. *SIAM J. Appl. Dyn. Syst.* **2017**, *16*, 546–596. [\[CrossRef\]](#)
41. Krupa, M.; Wechselberger, M. Local analysis near a folded saddle-node singularity. *J. Differ. Equ.* **2010**, *248*, 2841–2888. [\[CrossRef\]](#)
42. Vo, T.; Wechselberger, M. Canards of folded saddle-node type I. *SIAM J. Math. Anal.* **2015**, *47*, 3235–3283. [\[CrossRef\]](#)
43. Milik, A.; Szmolyan, P. Multiple time scales and canards in a chemical oscillator. In *Multiple-Time-Scale Dynamical Systems*; Jones, C.K.R.T., Khibnik, A.I., Eds.; Springer: New York, NY, USA, 2001; pp. 117–140.
44. Guckenheimer, J. Singular hopf bifurcation in systems with two slow variables. *SIAM J. Appl. Dyn. Syst.* **2008**, *7*, 1355–1377. [\[CrossRef\]](#)
45. Brøns, M.; Kaasen, R. Canards and mixed-mode oscillations in a forest pest model. *Theor. Popul. Biol.* **2010**, *77*, 238–242. [\[CrossRef\]](#)
46. Brøns, M.; Desroches, M.; Krupa, M. Mixed-mode oscillations due to a singular hopf bifurcation in a forest pest model. *Math. Popul. Stud.* **2015**, *22*, 71–79. [\[CrossRef\]](#)
47. Shchurov, I. Canard cycles in generic fast-slow systems on the torus. *T. Mosc. Math. Soc.* **2010**, *71*, 175–207. [\[CrossRef\]](#)
48. Kramer, M.A.; Traub, R.D.; Kopell, N.J. New dynamics in cerebellar Purkinje cells: Torus canards. *Phys. Rev. Lett.* **2008**, *101*, 068103. [\[CrossRef\]](#)
49. Benes, G.N.; Barry, A.M.; Kaper, T.J.; Kramer, M.A.; Burke, J. An elementary model of torus canards. *Chaos* **2011**, *21*, 023131. [\[CrossRef\]](#)
50. Desroches, M.; Burke, J.; Kaper, T.J.; Kramer, M.A. Canards of mixed type in a neural burster. *Phys. Rev. E* **2012**, *85*, 021920. [\[CrossRef\]](#)
51. Burke, J.; Desroches, M.; Barry, A.M.; Kaper, T.J.; Kramer, M.A. A showcase of torus canards in neuronal bursters. *J. Math. Neurosci.* **2012**, *2*, 3. [\[CrossRef\]](#)
52. Malashchenko, T.; Shilnikov, A.; Cymbalyuk, G. Six types of multistability in a neuronal model based on slow calcium current. *PLoS ONE* **2011**, *6*, e21782. [\[CrossRef\]](#) [\[PubMed\]](#)
53. Ju, H.; Neiman, A.B.; Shilnikov, A.L. Bottom-up approach to torus bifurcation in neuron models. *Chaos* **2018**, *28*, 106317. [\[CrossRef\]](#)
54. Wojcik, J.; Shilnikov, A. Voltage interval mappings for activity transitions in neuron models for elliptic bursters. *Phys. D* **2011**, *240*, 1164–1180. [\[CrossRef\]](#)
55. Shilnikov, A.; Cymbalyuk, G. Transition between tonic spiking and bursting in a neuron model via the blue-sky catastrophe. *Phys. Rev. Lett.* **2005**, *94*, 048101. [\[CrossRef\]](#) [\[PubMed\]](#)
56. Roberts, K.L.; Rubin, J.E.; Wechselberger, M. Averaging, folded singularities, and torus canards: Explaining transitions between bursting and spiking in a coupled neuron model. *SIAM J. Appl. Dyn. Syst.* **2015**, *14*, 1808–1844. [\[CrossRef\]](#)
57. Brøns, M. *Canards and Excitability in Liénard Equations*; Department of Mathematics, Denmark's Technical College: Lyngby, Denmark, 1989.
58. Desroches, M.; Krupa, M.; Rodrigues, S. Inflection, canards and excitability threshold in neuronal models. *J. Math. Biol.* **2013**, *67*, 989–1017. [\[CrossRef\]](#)
59. Kuehn, C. From first Lyapunov coefficients to maximal canards. *Int. J. Bifurcat. Chaos* **2010**, *20*, 1467–1475. [\[CrossRef\]](#)
60. Rotstein, H.G.; Kuske, R. Localized and asynchronous patterns via canards in coupled calcium oscillators. *Phys. D* **2006**, *215*, 46–61. [\[CrossRef\]](#)
61. Drover, J.; Rubin, J.; Su, J.; Ermentrout, B. Analysis of a canard mechanism by which excitatory synaptic coupling can synchronize neurons at low firing frequencies. *SIAM J. Appl. Math.* **2004**, *65*, 69–92. [\[CrossRef\]](#)
62. Ermentrout, B.; Wechselberger, M. Canards, clusters, and synchronization in a weakly coupled interneuron model. *SIAM J. Appl. Dyn. Syst.* **2009**, *8*, 253–278. [\[CrossRef\]](#)
63. Sekikawa, M.; Inaba, N.; Yoshinaga, T.; Hikiyara, T. Period-doubling cascades of canards from the extended Bonhoeffer–van der Pol oscillator. *Phys. Lett. A* **2010**, *374*, 3745–3751. [\[CrossRef\]](#)
64. Nakano, H.; Honda, H.; Okazaki, H. Canards in a slow-fast continuous piecewise linear vector field. *J. Anat.* **2005**, *105*, 381–382.
65. Itoh, M.; Murakami, H. Chaos and canards in the van der Pol equation with periodic forcing. *Int. J. Bifurcat. Chaos* **1994**, *4*, 1023–1029. [\[CrossRef\]](#)
66. Brøns, M.; Krupa, M.; Wechselberger, M. Mixed mode oscillations due to the generalized canard phenomenon. *Fields Inst. Commun.* **2006**, *49*, 39–63.
67. Itoh, M.; Chua, L.O. Canards and chaos in nonlinear systems. *IEEE Int. Symp. Circuits Syst.* **1992**, *6*, 2789–2792.
68. Rubin, J.; Wechselberger, M. Giant squid-hidden canard: The 3D geometry of the Hodgkin-Huxley model. *Biol. Cybern.* **2007**, *97*, 5–32. [\[CrossRef\]](#)
69. Moehlis, J. Canards for a reduction of the Hodgkin-Huxley equations. *J. Math. Biol.* **2006**, *52*, 141–153. [\[CrossRef\]](#)

70. Sowers, R.B. Random perturbations of canards. *J. Theor. Probab.* **2008**, *21*, 824–889. [\[CrossRef\]](#)
71. Zhezherun, A.A.; Pokrovskii, A.V. Topological method for analysis of periodic canards. *Automat. Rem. Contr.* **2009**, *70*, 967–981. [\[CrossRef\]](#)
72. Durham, J.; Moehlis, J. Feedback control of canards. *Chaos* **2008**, *18*, 015110. [\[CrossRef\]](#) [\[PubMed\]](#)
73. Valero, M.; Zutshi, I.; Yoon, E.; Buzsaki, G. Probing subthreshold dynamics of hippocampal neurons by pulsed optogenetics. *Science* **2022**, *375*, 570–574. [\[CrossRef\]](#) [\[PubMed\]](#)
74. Hodgkin, A.L.; Huxley, A.F. A quantitative description of membrane current and its application to conduction and excitation in nerve. *J. Physiol.* **1952**, *117*, 500–544. [\[CrossRef\]](#)
75. Hodgkin, A.L.; Huxley, A.F. Current carried by sodium and potassium ions through the membrane of the giant axon of Loligo. *J. Physiol.* **1952**, *116*, 449–472. [\[CrossRef\]](#)
76. Hodgkin, A.L.; Huxley, A.F. The components of membrane conductance in the giant axon of Loligo. *J. Physiol.* **1952**, *116*, 473–496. [\[CrossRef\]](#)
77. Hodgkin, A.L.; Huxley, A.F. The dual effect of membrane potential on sodium conductance in the giant axon of Loligo. *J. Physiol.* **1952**, *116*, 497–506. [\[CrossRef\]](#)
78. Fitzhugh, R. Impulses and physiological states in theoretical models of nerve membrane. *Biophys. J.* **1961**, *1*, 445–466. [\[CrossRef\]](#)
79. Nagumo, J.; Arimoto, S.; Yoshizawa, S. An active pulse transmission line simulating a nerve axon. *Proc. IRE* **1962**, *50*, 2061–2070. [\[CrossRef\]](#)
80. Morris, C.; Lecar, H. Voltage oscillations in the barnacle giant muscle fiber. *Biophys. J.* **1981**, *35*, 193–213. [\[CrossRef\]](#)
81. Hindmarsh, J.L.; Rose, R.M. A model of neuronal bursting using three coupled first order differential equations. *Proc. R. Soc. Lond. B Biol. Sci.* **1984**, *221*, 87–102. [\[PubMed\]](#)
82. Rinzel, J. Excitation dynamics: Insights from simplified membrane models. *Fed. Proc.* **1986**, *44*, 2944–2946.
83. Rinzel, J. Bursting oscillations in an excitable membrane model. In *Ordinary and Partial Differential Equations*; Brian, D.S., Richard, J.J., Eds.; Springer: Berlin/Heidelberg, Germany, 1985.
84. Rinzel, J.; Lee, Y.S. Dissection of a model for neuronal parabolic bursting. *J. Math. Biol.* **1987**, *25*, 653–675. [\[CrossRef\]](#) [\[PubMed\]](#)
85. Sherman, A.; Rinzel, J. Rhythmogenic effects of weak electrotonic coupling in neuronal models. *Proc. Nat. Acad. Sci. USA* **1992**, *89*, 2471–2474. [\[CrossRef\]](#)
86. Av-Ron, E.; Parnas, H.; Segel, L.A. A basic biophysical model for bursting neurons. *Biol. Cybern.* **1993**, *69*, 87–95. [\[CrossRef\]](#)
87. Holden, L.; Erneux, T. Slow passage through a hopf bifurcation: From oscillatory to steady state solutions. *SIAM J. Appl. Math.* **1993**, *53*, 1045–1058. [\[CrossRef\]](#)
88. Holden, L.; Erneux, T. Understanding bursting oscillations as periodic slow passages through bifurcation and limit points. *J. Math. Biol.* **1993**, *31*, 351–365. [\[CrossRef\]](#)
89. Rush, M.E.; Rinzel, J. Analysis of bursting in a thalamic neuron model. *Biol. Cybern.* **1994**, *71*, 281–291. [\[CrossRef\]](#)
90. Smolen, P.; Terman, D.; Rinzel, J. Properties of a bursting model with two slow inhibitory variables. *SIAM J. Appl. Math.* **1993**, *53*, 861–892. [\[CrossRef\]](#)
91. Pernarowski, M. Fast subsystem bifurcations in a slowly varying Liénard system exhibiting bursting. *SIAM J. Appl. Math.* **1994**, *54*, 814–832. [\[CrossRef\]](#)
92. Izhikevich, E.M. Neural excitability, spiking and bursting. *Int. J. Bifurcat. Chaos* **2000**, *10*, 1171–1266. [\[CrossRef\]](#)
93. Izhikevich, E.M.; Hoppensteadt, F. Classification of bursting mappings. *Int. J. Bifurcat. Chaos* **2004**, *14*, 3847–3854. [\[CrossRef\]](#)
94. Izhikevich, E.M. *Dynamical Systems in Neuroscience: The Geometry of Excitability and Bursting*; MIT Press: Cambridge, MA, USA, 2007.
95. Lu, B.; Liu, S.; Jiang, X.; Wang, X. Bifurcation and spike adding transition in Chay-Keizer model. *Int. J. Bifurcat. Chaos* **2016**, *26*, 1650090. [\[CrossRef\]](#)
96. Wang, J.; Liu, S.; Liu, X.; Zeng, Y. Bifurcation and firing patterns of the pancreatic  $\beta$ -Cell. *Int. J. Bifurcat. Chaos* **2015**, *25*, 1530024. [\[CrossRef\]](#)
97. Wang, J.; Lu, B.; Liu, S.; Jiang, X. Bursting types and bifurcation analysis in the pre-Bötzinger complex respiratory rhythm neuron. *Int. J. Bifurcat. Chaos* **2017**, *27*, 1750010. [\[CrossRef\]](#)
98. Zhan, F.; Liu, S.; Wang, J.; Lu, B. Bursting patterns and mixed-mode oscillations in reduced Purkinje model. *Int. J. Mod. Phys. B* **2018**, *32*, 1850043. [\[CrossRef\]](#)
99. Yang, Z.; Lu, Q. Different types of bursting in Chay neuronal model. *Sci. China Ser. G* **2008**, *51*, 687–698. [\[CrossRef\]](#)
100. Desroches, M.; Rinzel, J.; Rodrigues, S. Classification of bursting patterns: A tale of two ducks. *PLoS Comput. Biol.* **2022**, *18*, e1009752. [\[CrossRef\]](#)
101. Ersoz, E.K.; Desroches, M.; Krupa, M.; Clement, F. Canard-mediated (De)synchronization in coupled phantom bursters. *SIAM J. Appl. Dyn. Syst.* **2016**, *15*, 580–608. [\[CrossRef\]](#)
102. Hasan, C.R.; Krauskopf, B.; Osinga, H.M. Saddle slow manifolds and canard orbits in  $R^4$  and application to the full Hodgkin–Huxley model. *J. Math. Neurosci.* **2018**, *8*, 5. [\[CrossRef\]](#)
103. Albizuri, J.U.; Desroches, M.; Krupa, M.; Rodrigues, S. Inflection, canards and folded singularities in excitable systems: Application to a 3D FitzHugh–Nagumo model. *J. Nonlinear Sci.* **2020**, *30*, 3265–3291. [\[CrossRef\]](#)
104. Desroches, M.; Kowalczyk, P.; Rodrigues, S. Spike-adding and reset-induced canard cycles in adaptive integrate and fire models. *Nonlinear Dyn.* **2021**, *104*, 2451–2470. [\[CrossRef\]](#)

105. Ersoz, E.K.; Desroches, M.; Krupa, M. Synchronization of weakly coupled canard oscillators. *Phys. D* **2017**, *349*, 46–61. [\[CrossRef\]](#)
106. Desroches, M.; Kirk, V. Spike-adding in a canonical three-time-scale model: Superslow explosion and folded-saddle canards. *SIAM J. Appl. Dyn. Syst.* **2018**, *17*, 1989–2017. [\[CrossRef\]](#)
107. Ersoz, E.K.; Desroches, M.; Guillamon, A.; Rinzel, J.; Tabak, J. Canard-induced complex oscillations in an excitatory network. *J. Math. Biol.* **2020**, *80*, 2075–2107. [\[CrossRef\]](#) [\[PubMed\]](#)
108. Lizarraga, I.; Wechselberger, M. Computational singular perturbation method for nonstandard slow-fast systems. *SIAM J. Appl. Dyn. Syst.* **2020**, *19*, 994–1028. [\[CrossRef\]](#)
109. Wechselberger, M. Geometric Singular Perturbation Theory beyond the Standard Form. In *Frontiers in Applied Dynamical Systems: Reviews and Tutorials*; Springer: Berlin/Heidelberg, Germany, 2020; Volume 6.
110. Jelbart, S.; Pages, N.; Kirk, V.; Sneyd, J.; Wechselberger, M. Process-oriented geometric singular perturbation theory and calcium dynamics. *SIAM J. Appl. Dyn. Syst.* **2022**, *21*, 982–1029. [\[CrossRef\]](#)
111. Booth, V.; Carr, T.W.; Erneux, T. Near-threshold bursting is delayed by a slow passage near a limit point. *SIAM J. Appl. Math.* **1997**, *57*, 1406–1420.
112. Baer, S.M.; Erneux, T.; Rinzel, J. The slow passage through a hopf bifurcation: Delay, memory effects, and resonance. *SIAM J. Appl. Math.* **1989**, *49*, 55–71. [\[CrossRef\]](#)
113. Neishtadt, A.I. Persistence of stability loss for dynamical bifurcations I. *Diff. Equ.* **1987**, *23*, 1385–1391.
114. Neishtadt, A.I. Persistence of stability loss for dynamical bifurcations II. *Diff. Equ.* **1988**, *24*, 171–176.
115. Larter, R.; Steinmetz, C.G. Chaos via mixed-mode oscillations. *Philos. Trans. R. Soc. A* **1991**, *337*, 291–298.
116. Koper, M.T.M. Bifurcations of mixed-mode oscillations in a three-variable autonomous Van der Pol-Duffing model with a cross-shaped phase diagram. *Phys. D* **1995**, *80*, 72–94. [\[CrossRef\]](#)
117. Arneodo, A.; Argoul, F.; Elezgaray, J.; Richetti, P. Homoclinic chaos in chemical systems. *Phys. D* **1993**, *62*, 134–169. [\[CrossRef\]](#)
118. Guckenheimer, J.; Harris-Warrick, R.; Peck, J.; Willms, A. Bifurcation, bursting, and spike frequency adaptation. *J. Comput. Neurosci.* **1997**, *4*, 257–277. [\[CrossRef\]](#)
119. Guckenheimer, J.; Willms, A.R. Asymptotic analysis of subcritical Hopf–Homoclinic bifurcation. *Phys. D* **2000**, *139*, 195–216. [\[CrossRef\]](#)
120. Desroches, M.; Guckenheimer, J.; Krauskopf, B.; Kuehn, C.; Osinga, H.M.; Wechselberger, M. Mixed-mode oscillations with multiple time scales. *SIAM Rev.* **2012**, *54*, 211–288. [\[CrossRef\]](#)
121. Lu, B.; Liu, S.; Liu, X. Advances in the dynamics of mixed mode oscillations in neuron models (In Chinese). *J. Dynam. Control* **2016**, *14*, 481–491.
122. Lu, B.; Liu, S.; Jiang, X.; Wang, J.; Wang, X. The mixed-mode oscillations in Av-Ron-Parnas-Segel model. *Discret. Contin. Dyn. Syst.* **2017**, *10*, 487–504. [\[CrossRef\]](#)
123. Zhan, F.; Liu, S.; Zhang, X.; Wang, J.; Lu, B. Mixed-mode oscillations and bifurcation analysis in a pituitary model. *Nonlinear Dynam.* **2018**, *94*, 807–826. [\[CrossRef\]](#)
124. Ni, M. *Asymptotic Theory in Singular Perturbation Problems*; Higher Education Press: Beijing, China, 2009. (In Chinese)
125. Takens, F. Constrained equations; a study of implicit differential equations and their discontinuous solutions. In *Structural Stability, the Theory of Catastrophes, and Applications in the Sciences*; Hilton, P., Ed.; Springer: Berlin/Heidelberg, Germany, 1976; pp. 143–234.
126. Kuznetsov, Y.A. *Elements of Applied Bifurcation Theory*; Springer: New York, NY, USA, 1998.
127. Lu, B. Mixed Mode Oscillations and Dynamics of Neurons. Master's Thesis, South China University of Technology, Guangzhou, China, 2016. (In Chinese)
128. Desroches, M.; Kaper, T.J.; Krupa, M. Mixed-mode bursting oscillations: Dynamics created by a slow passage through spike-adding canard explosion in a square-wave burster. *Chaos* **2013**, *23*, 046106. [\[CrossRef\]](#) [\[PubMed\]](#)
129. Best, J.; Borisjuk, A.; Rubin, J.; Terman, D.; Wechselberger, M. The dynamic range of bursting in a model respiratory pacemaker network. *SIAM J. Appl. Dyn. Syst.* **2005**, *4*, 1107–1139. [\[CrossRef\]](#)
130. Shilnikov, A.; Shilnikov, L.; Turaev, D. Blue sky catastrophe in singularly perturbed systems. *Mosc. Math. J.* **2005**, *5*, 269–282. [\[CrossRef\]](#)
131. Shilnikov, A.; Calabrese, R.L.; Cymbalyuk, G. Mechanism of bistability: Tonic spiking and bursting in a neuron model. *Phys. Rev. E* **2005**, *71*, 056214. [\[CrossRef\]](#)
132. Shilnikov, A.; Cymbalyuk, G. Homoclinic bifurcations of periodic orbits on a route from tonic spiking to bursting in neuron models. *Regul. Chaotic Dyn.* **2004**, *9*, 281–297. [\[CrossRef\]](#)
133. Cymbalyuk, G.; Shilnikov, A. Coexistence of tonic spiking oscillations in a leech neuron model. *J. Comput. Neurosci.* **2005**, *18*, 255–263. [\[CrossRef\]](#)
134. Cymbalyuk, G.S.; Calabrese, R.L.; Shilnikov, A.L. How a neuron model can demonstrate co-existence of tonic spiking and bursting. *Neurocomputing* **2005**, *65–66*, 869–875. [\[CrossRef\]](#)
135. Malashchenko, T.; Shilnikov, A.; Cymbalyuk, G. Bistability of bursting and silence regimes in a model of a leech heart interneuron. *Phys. Rev. E* **2011**, *84*, 041910. [\[CrossRef\]](#)
136. Pontryagin, L.S.; Rodygin, L.V. Periodic solution of a system of ordinary differential equations with a small parameter in the terms containing derivatives. *Sov. Math. Dokl.* **1960**, *1*, 611–614.

137. Zhan, F.; Su, J.; Liu, S. Canards dynamics to explore the rhythm transition under electromagnetic induction. *Chaos Solitons Fractals* **2023**, *169*, 113304. [[CrossRef](#)]
138. Yu, H.; Chen, Y. Some advances in dimensionality reduction methods for higher dimensional nonlinear dynamic systems. *Adv. Mech.* **2009**, *39*, 154–164. (In Chinese)

**Disclaimer/Publisher's Note:** The statements, opinions and data contained in all publications are solely those of the individual author(s) and contributor(s) and not of MDPI and/or the editor(s). MDPI and/or the editor(s) disclaim responsibility for any injury to people or property resulting from any ideas, methods, instructions or products referred to in the content.